

Vibrational analysis of benitoite ($\text{BaTiSi}_3\text{O}_9$) and the Si_3O_9 ring

Charles C. Kim and M. I. Bell

Naval Research Laboratory, Dynamics of Solids Branch, Code 6680, Washington, D.C. 20375-5320

D. A. McKeown*

Department of Chemistry, Howard University, Washington, D.C. 20059

(Received 19 October 1992)

The normal modes of vibration and their frequencies are calculated for benitoite, a mineral whose crystal structure (space group D_{3h}^2) consists of three-membered silicate rings (Si_3O_9) linked by Ba^{2+} and Ti^{4+} ions. Factor-group analysis dictates that certain normal modes involve the motion of only the ring atoms. On the assumption that mode mixings and splittings due to inter-ring interactions are small, the normal frequencies of the isolated ring of C_{3h} symmetry are determined by fitting to suitable averages of selected frequencies in the Raman spectra. A valence force potential consisting of only central interactions between nearest neighbors and bond-bending interactions centered at the silicon atoms is used. This potential is then extended to the full crystal structure by including interactions involving the Ba^{2+} and Ti^{4+} ions. The frequencies obtained are in excellent agreement with the infrared and Raman spectra, requiring only minor adjustment of the force constants obtained for the isolated ring. The identification of normal modes characteristic of three-membered silicate rings may prove to be a valuable guide in the interpretation of the infrared and Raman spectra of amorphous silicates, potentially leading to new information on the ring statistics of these materials.

I. INTRODUCTION

Cyclosilicates¹ are minerals containing a single type of three-, four-, or six-membered silicate ring. Several experimental studies of their vibrational spectra have been reported.^{2,3} More work needs to be done, however, to relate the observed spectra to the dynamics of the rings and their coupling within the crystal structure. A better understanding of the vibrational spectra of cyclosilicates may be useful in characterizing the vibrational spectra of crystalline and amorphous⁴ silicates which contain rings. Furthermore, this knowledge can aid in understanding the vibrational spectra of other silicates with different polymerization of the silicate tetrahedra.

Benitoite ($\text{BaTiSi}_3\text{O}_9$) is a cyclosilicate containing rings of three linked tetrahedra (Si_3O_9). It belongs to the space group $P\bar{6}c2$ (D_{3h}^2) and has two formula units per unit cell.⁵ Figure 1 shows the crystal structure, where each ring is shown as composed of tetrahedral units. The rings are located one above the other along the c axis. The c axis passing through the origin is the axis of threefold symmetry. Twofold symmetry axes are perpendicular to the c axis, pass through the origin, and through the Ba and Ti ions. The two rings are symmetrical with respect to rotation about the twofold axis. The c axis and one of twofold symmetry axes are designated as the z and x axes, respectively.

The infrared reflectance spectrum of benitoite was first reported by Matossi and Krüger.⁶ The Raman spectrum of benitoite in powder form was first reported by Griffith.⁷ Adams and Gardner⁸ presented the Raman and infrared reflectance spectra of single-crystal benitoite. They were able to show almost all of the lines predicted

from the factor group analysis, and assign their symmetry species quite unambiguously. Recently, we again measured the Raman and infrared spectra of benitoite single crystals^{9,10} and observed frequencies which are consistently lower by 12 cm^{-1} than those reported in Ref. 8. For reasons indicated below and discussed at length

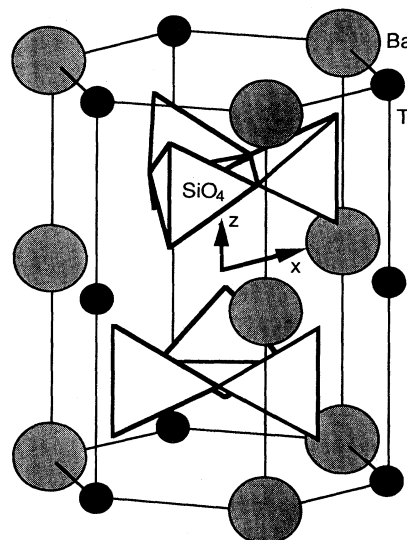


FIG. 1. Schematic diagram of the structure of benitoite. The rings are shown as three linked tetrahedra. The c axis is the threefold symmetry axis and is set to be the z axis. The twofold symmetry axis is along the line connecting Ba to Ti in the ab plane and is set to be the x axis.

elsewhere,⁹ we have used our results in the normal mode calculations.

Although the vibrational spectra of benitoite are known, no normal mode analysis has been reported. Matossi¹¹ and Saksena, Agarwal, and Jauhri¹² calculated the normal frequencies of the silicate ring (Si_3O_9) in benitoite, assuming its symmetry to be D_{3h} . Later, it was discovered⁵ that the ring actually has C_{3h} symmetry; the normal frequencies of a ring with this symmetry have not yet been calculated. Furthermore, mode splittings due to interactions between the rings (Davydov splitting^{13,14}) prevent direct comparison between calculated and observed frequencies. We have performed the first complete normal coordinate analysis of benitoite. It enables us to assign normal modes to the observed frequencies and to determine the magnitudes of atomic interactions between the rings through the cations.

We present the normal coordinate analysis in two steps. First, we treat the Si_3O_9 ring as an isolated molecule and obtain its normal modes and frequencies. Next, we calculate the lattice dynamics of benitoite at zero wave vector and describe the results. The values of the force constants obtained for the isolated ring are essential in obtaining the reasonable values of the force constants for the crystal. In the fitting procedure, it is important to use reasonable initial values to avoid spurious results due to false minima. The values of the force constants determined for the isolated ring provide good initial values of the force constants for the crystal. This approach is justified because the strength of the coupling between the rings is known to be less than that among the atoms in the ring. More importantly, we want to find the representative vibrational frequencies of the isolated ring and establish the relationship between the vibrational frequencies of the ring and those of the crystal. Knowledge of this relationship may be essential in understanding the vibrational spectra of amorphous silicates containing rings.

In Sec. II, we explain briefly the method used in the normal coordinate analysis of the isolated ring and the crystal. In Sec. III, we present our results for the isolated ring and in Sec. IV for the full crystal structure. In Sec. V, we discuss several implications of our results in the study of crystalline and amorphous silicates.

II. METHOD OF CALCULATION AND FIT

Normal mode analysis for crystals is well described by a number of authors.¹⁵⁻¹⁷ Customarily, the analysis of the crystal is accomplished by constructing the dynamical matrix D . On the other hand, calculations for molecules are most often performed using Wilson's FG matrix^{18,19} or related methods.²⁰ In this study, the dynamical matrix was constructed not only for the crystal, but also for the Si_3O_9 ring because the D matrix can be simply and systematically block diagonalized. The block diagonalization is essential for two reasons. First, it determines the species of the calculated normal frequencies. Otherwise, one has to manipulate each corresponding normal mode to determine its species, a process which becomes tedious and time consuming as the total number of the

atoms in the system increases. More importantly, fitting the calculated frequencies to the observed frequencies *species by species* is impossible without the block diagonalization. Block diagonalization is valuable when (i) the total number of the frequencies is large, (ii) the modes of different species are too close to be distinguished by their frequencies alone, and (iii) the frequencies of selected species must be used for the fit. In the present work, the last of these advantages is essential.

We describe briefly how to obtain the normal frequencies and modes. We set η and ξ as the displacement vectors with respect to the equilibrium positions of the atoms in the Cartesian and internal coordinate systems, respectively. The dimensions of η and ξ are $3N$ and M , respectively, where N is the total number of the atoms and M is the total number of internal coordinates in the system. We find the B matrix which transforms η into ξ using the relation

$$\xi = B\eta. \quad (1)$$

Note that B has dimension $M \times 3N$ and may in general be singular. Construction¹⁶ of B is straightforward for a molecule, but requires the summation over several unit cells for a crystal structure. The potential energy V for a given system can be easily constructed by the use of ξ as follows:

$$V = \frac{1}{2} \sum_{i \geq j} k_{ij} \xi_i \xi_j, \quad (2)$$

where ξ_i is the i th component of ξ and k_{ij} is the force constant. We assume a valence force potential consisting of only central interactions between nearest neighbors and bond-bending interactions. Hence, $k_{ij} = k_{ij} \delta_{ij}$ where δ_{ij} is the conventional Kronecker delta. The determination of V leads to the construction of the dynamical matrix,

$$D = G^{\frac{1}{2}} B^T F B G^{\frac{1}{2}}, \quad (3)$$

where $F_{ij} = k_{ij}$ and G is the inverse of the diagonal matrix whose diagonal component is the atomic mass. The normal frequencies and normal modes can be obtained from the eigenvalues and eigenvectors of D . However, those solutions do not identify the corresponding species. Thus, we proceed to find the unitary matrix U , which block diagonalizes the D matrix and leads to the block diagonalized matrix,²¹

$$D' = U^\dagger D U. \quad (4)$$

Then, the eigenvalue solution of D' by

$$D' e'_i = \omega_i^2 e'_i \quad (5)$$

produces the normal frequency ω_i . The atomic displacement vector

$$e_i = G^{\frac{1}{2}} U e'_i \quad (6)$$

presents the normal mode corresponding to ω_i .

We have developed a FORTRAN program which calculates D from the positions and masses of the atoms in the system and from the atomic interactions specified for the

given system. The program also block diagonalizes D by constructing U automatically²² by imposing the orthogonality condition among the projection vectors²³ obtained for each species. It also determines the force constants by minimizing the relative mean-square error

$$\sigma^2 = \sum_{\mu} \sum_{i=1}^{N_{\mu}} \left(1 - \frac{\omega_{i,\mu}^{\text{cal}}}{\omega_{i,\mu}^{\text{obs}}} \right)^2, \quad (7)$$

where μ refers to the species, N_{μ} is the total number of observed frequencies for the species μ , and $\omega_{i,\mu}^{\text{cal}}$ and $\omega_{i,\mu}^{\text{obs}}$ are the calculated and observed frequencies, respectively.

III. NORMAL COORDINATE ANALYSIS OF THE SILICATE RING

Figure 2 shows the structure of the Si₃O₉ ring in benitoite. The atomic positions are obtained from Fischer⁵ who refined the atomic positions of benitoite reported earlier by Zachariassen.²⁴ Note the three different Si-O distances, each of which differs slightly from the grand average of 1.62 Å. The common reference frame for the ring is the same as that defined for the crystal (Fig. 1) except that the origin is shifted along the c axis to be at the center of the ring. The ring is viewed as three linked SiO₄ tetrahedra. Each tetrahedron has two bridging oxygen atoms, designated O(1), which are shared with two neighboring tetrahedra, and two nonbridging oxygen atoms, designated O(2). The selection rules for the Si₃O₉ ring are shown in Table I. The isolated ring has C_{3h} symmetry and its irreducible representation is $6A' + 4A'' + 6E' + 4E''$. The total number of vibrational frequencies is 20.

The first step in the normal coordinate analysis is the construction of V . Table II shows the nature of force constants used in constructing V . The Si-O(1) stretching force constant κ_1 can be further divided into two separate force constants, κ_s and κ_l , where the subscripts s and l signify the shorter and longer bond lengths between Si and O(1), respectively. We find, however, that this division does not improve the fit significantly, and we therefore set $\kappa_1 = \kappa_s = \kappa_l$. It is worthwhile to mention the bond-bending force constant (κ_3) centered at Si. In the crystal structure of benitoite, the O(2) bonding is more ionic than that of O(1). In light of this picture, κ_3 may be further divided. At this stage of the calculation, we treat the ring in benitoite as the isolated molecule assuming that there are no interactions between the ring and the surrounding atoms. For this reason, we treat equally all of bond-bending force constants centered at Si. The potential energy (V_1) for a tetrahedron composed

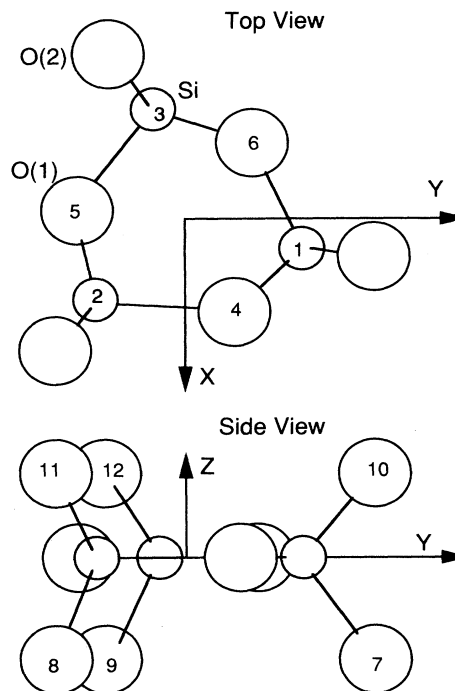


FIG. 2. Schematic diagram of the Si₃O₉ ring with the same reference frame in Fig. 1, except that the origin is shifted to be at the center of the ring. The atoms are numbered for the sake of identification in describing the potential energy.

of atoms 1, 4, 6, 7, and 10 (see Fig. 2 for the numbering) has the form

$$2V_1 = \kappa_1 (r_{1,4}^2 + r_{1,6}^2) + \kappa_2 (r_{1,7}^2 + r_{1,10}^2) + \kappa_3 (\delta_{4,1,6}^2 + \delta_{4,1,7}^2 + \delta_{6,1,7}^2 + \delta_{4,1,10}^2 + \delta_{6,1,10}^2 + \delta_{7,1,10}^2), \quad (8)$$

where $r_{\mu,\nu}$ is the change in bond length between atoms μ and ν , and $\delta_{\mu,\nu,\gamma}$ is the change in bond angle at atom ν for the triangle composed of atoms μ , ν , and γ . The potential energies V_2 and V_3 for the other two tetrahedra are constructed in the same way as in Eq. (8) and are added together to produce the potential energy

$$V_{\text{ring}} = V_1 + V_2 + V_3 \quad (9)$$

for the Si₃O₉ ring.

For V_{ring} , each of the V_i 's contains 10 internal coordinates, but provides only 9 independent internal coor-

TABLE I. The irreducible representations of the Si₃O₉ ring and benitoite. The number for each species is the number of the normal frequencies or modes. The acoustic modes $A'' + E'$ are included for benitoite. R and IR inside the parentheses refer to Raman active and infrared active species, respectively.

Structure	Species			
Ring (C_{3h})	$6A'(\text{R})$	$4A''(\text{IR})$	$6E'(\text{R, IR})$	$4E''(\text{R})$
Benitoite (D_{3h})	$7A'_1(\text{R}) + 9A'_2$	$5A'_1 + 7A'_2(\text{IR})$	$16E'(\text{R, IR})$	$12E''(\text{R})$

TABLE II. The nature and values of the force constants for the Si_3O_9 ring. O includes both O(1) and O(2).

	κ_1 (10^5 dyne/cm) Si-O(1) stretch	κ_2 (10^5 dyne/cm) Si-O(2) stretch	κ_3 (10^{-11} erg) O-Si-O bend
Present work	4.2	4.3	1.5
Ref. 12	4.0	5.0	1.8 ^a

^a $\kappa_3/d^2 = 0.7 \times 10^5$ dyne/cm where $d = 1.6 \text{ \AA}$ is the average Si-O bond length.

dinates since one of internal coordinates is linearly dependent on the others.¹⁶ Nevertheless, each V_i provides the complete set of internal coordinates for a tetrahedron, since 9 vibrational frequencies are expected for each tetrahedron. On the other hand, V_{ring} does not provide the complete set of internal coordinates. For the ring, 20 vibrational frequencies are expected from the symmetry analysis. Equation (9) shows that V_{ring} has only 27 independent internal coordinates, which leads to only 18 vibrational frequencies. As a result, one vibrational frequency of species A'' and another of species E'' have the value of zero. Including more interactions such as the direct interaction²⁵ between O(2) in one tetrahedron and O(2) in another tetrahedron provides the complete set of internal coordinates for the ring. However, those interactions are not physical, since the corresponding atoms are not directly bonded to each other. For this reason, we use Eq. (9) without including more interactions.

The values of the force constants are determined by fitting the calculated frequencies to the observed frequencies. Two problems arise. First, the calculated frequencies are obtained for the isolated ring, whereas the observed frequencies are obtained from the vibrational spectra of benitoite. The calculation yields neither the pairs of lines (Davydov splitting^{13,14}) due to the coupling of the rings through Ba and Ti ions in benitoite, nor the external vibrational modes due to the motions of Ba and Ti or rigid rotation or translation of the rings. Secondly, some of the vibrational spectra of benitoite contain LO-TO shifts, whereas our calculation does not take this effect into account. We adopt the following ideas to minimize the problems. It is believed that the highest frequencies in the vibrational spectra of benitoite most closely represent the internal vibrations of the ring. For this reason, we select to fit the highest frequencies available from the vibrational spectra of benitoite. For pairs of frequencies that are apparently due to Davydov splitting, their average can be used for the fitting, that is

$$\bar{\omega} = \sqrt{\frac{\omega_+^2 + \omega_-^2}{2}}, \quad (10)$$

where ω_+ and ω_- are the higher and lower frequencies, respectively, for each Davydov pair. We fit the vibrational frequencies of only the A'_1 and E'' species, simply because these frequencies do not have LO-TO shifts. At least three observed frequencies are necessary to determine three unknown force constants. Since the fitting with three frequencies becomes unstable due to the non-

linearity of Eq. (7), we choose the four observed frequencies 1048 cm^{-1} (A'_1), 917 cm^{-1} (A'_1), 628 cm^{-1} (A'_1), and 932 cm^{-1} (E''), obtained from our Raman spectra⁹ and Eq. (10). The resulting values of the force constants are shown in Table II. Based on those values, the normal modes and frequencies of the ring are easily obtained. We believe that this approach is the best way to extract the vibrational frequencies of the ring molecule from the vibrational frequencies of benitoite.

Saksena, Agarwal, and Jauhri¹² performed a normal mode analysis of the Si_3O_9 ring, using symmetry coordinates. In their calculation, they assumed the symmetry of the ring to be D_{3h} and set all of the Si-O bond lengths equal to 1.6 \AA . The values of force constants were obtained in an effort to match the calculated frequencies to all of the observed frequencies of the infrared spectra of benitoite available at that time. Table II compares our force constant values with those previously reported.¹² While the values for κ_1 are in good agreement, this is not the case for κ_2 . We obtain κ_1 approximately equal to κ_2 , whereas they found κ_1 to be significantly less than κ_2 .

Saksena, Agarwal, and Jauhri¹² reported the frequencies of the A'' and E' species only. We believe there to be two minor errors in their calculation which affect the three lowest frequencies in the E' species. For this reason, we repeated the calculation, using the same model. The first column in Table III shows the normal frequencies. The second column in Table III shows our values of the normal frequencies of the ring with C_{3h} symmetry, the structure in Fig. 2, and the force constants in the second row in Table II. The differences between the first and second columns in Table III are large enough to be observed. Do these differences arise solely from the

TABLE III. Comparison of the calculated frequencies of the E' species of the Si_3O_9 ring with different symmetries. Our results are obtained from the force constants in the second row of Table II. The values are given in units of cm^{-1} .

Ref. 12 (corrected)	Present work	
D_{3h}	C_{3h}	D_{3h}
271	256	256
332	299	300
499	468	469
750	706	708
907	857	856
1083	1072	1071

symmetry difference? We test that hypothesis by calculating the normal frequencies of the E' species, assuming that the O(1) and O(2) atoms in Fig. 2 rotate around the origin to produce the point symmetry D_{3h} for the ring, while keeping the same force constants as for C_{3h} symmetry. The resulting frequencies are listed in the third column of Table III. The differences are of the order of 1 cm^{-1} . Thus, the differences in our frequencies and theirs are mainly due to the differences in the force constants, not in the symmetry.

IV. NORMAL COORDINATE ANALYSIS OF BENITOITE

The selection rules for benitoite are shown in Table I. The total number of optical frequencies is 54; half of them are nondegenerate, and the rest are doubly degenerate. Table I also shows the correlations of the species between the ring and the crystal. The correlation analysis indicates exactly how the coupling of rings in benitoite causes the Davydov splitting of the vibrational frequencies of the isolated ring. The nondegenerate modes of the isolated ring are correlated with two separate species of nondegenerate modes of the crystal, while the doubly degenerate modes of the ring are related to the same species of doubly degenerate modes. Thus, pairs of lines due to Davydov splitting are observed in the vibrational spectra of the E' and E'' species, but not in the spectra of the nondegenerate modes.^{8,9}

One way to simplify the normal coordinate analysis for a complex system is to separate²⁶ the lattice modes into internal and external modes. This approach is plausible if a group of atoms in the crystal acts as a structural unit that is relatively isolated from the surrounding atoms. It is generally accepted that Ba and Ti bonding to the rings in benitoite is weak with respect to the bonding within the rings,² which would justify a separation into modes internal and external to the rings. The external mode frequencies can be calculated from a suitable valence force potential by treating the rings as point ions.²⁷ This approach is not well suited to the present work, however. It yields only effective force constants between the rings and the Ba and Ti ions which link them. More specific knowledge of the interactions between these ions and the nonbridging oxygens will be needed in order to build our

understanding of structurally related crystals and glasses. Also, the Davydov splitting of the internal modes cannot be obtained from this model, making it impossible to verify the assumptions used above in describing the isolated ring. We therefore performed the vibrational analysis of the benitoite crystal structure without attempting to separate internal and external modes.

The crystal structure as shown in Fig. 1 is used to construct the potential energy by a method similar to that presented in the previous section for the isolated ring. Table IV describes the various terms in the valence force potential. Note that the bond bending at Si is now divided into three different interactions: k_5 , k_6 , and k_7 , corresponding to O(1)-Si-O(1), O(1)-Si-O(2), and O(2)-Si-O(2), respectively. These were treated separately, since the nature of the interaction at O(2) is more ionic than that at O(1). All the interactions of Si-O(2)-Ba, Si-O(2)-Ti, and Ba-O(2)-Ti, however, are treated equally, since the corresponding force constants are small. Of course, the fitting may improve as one introduces more force constants. At the same time, increasing the number of adjustable parameters can lead to unphysical results such as negative values of the force constants. The potential chosen for our analysis leads to physically reasonable values of the force constants and is sufficient to produce nonzero frequencies for all of the normal modes. As discussed in the previous section, only the observed frequencies of the A'_1 and E'' species were used in the fitting. Table IV shows the resulting values of the force constants. The Si-O(1) bond stretch (k_1) and Si-O(2) bond stretch (k_2) do not change much from the corresponding values κ_1 and κ_2 for the isolated ring. In other words, the bond strengths within the ring do not change much whether the ring is isolated or is subject to the crystal environment. This confirms that the vibrational spectra of benitoite can be described to a good approximation in terms of the isolated ring. The Ti-O(2) bond stretch (k_4) is stronger by about a factor of 3 than the Ba-O(2) bond stretch (k_3). This result is in agreement with the classification due to Lazarev² of Ti⁴⁺ and Ba²⁺ as medium-strong cations and weak cations, respectively. Adams and Gardner⁸ suggest that the Ba-O(2) bond stretch can be ignored compared with the Ti-O(2) bond stretch. This is true to a certain degree, since our results show that the Ba-O(2) bond stretch is smaller than the Ti-O(2) bond stretch

TABLE IV. The nature and values of the force constants for benitoite.

Force constant	Interaction	Present work
k_1	Si-O(1)	$4.2 \times 10^5 \text{ dyne/cm}$
k_2	Si-O(2)	4.1
k_3	Ba-O(2)	0.66
k_4	Ti-O(2)	1.6
k_5	O(1)-Si-O(1)	$0.74 \times 10^{-11} \text{ erg}$
k_6	O(1)-Si-O(2)	1.8
k_7	O(2)-Si-O(2)	1.3
k_8	O(2)-Ba-O(2)	0.12
k_9	O(2)-Ti-O(2)	0.45
k_{10}	Si-O(2)-Ba, Si-O(2)-Ti, Ba-O(2)-Ti	0.15

by a factor of 3. The Ba-O(2) bond stretch cannot be totally neglected, however, since the quality of the fit is significantly improved by introducing this interaction. The ratio of the bond-bending to bond-stretching forces provides a measure of the ionicity or covalency of the bonding. The values of the force constants in Table IV indicate that the nature of the Si-O bond is the most covalent, followed by the Ti-O and Ba-O bonds.

Figures 3 and 4 show the calculated frequencies for the isolated ring, those for the benitoite crystal, and the observed frequencies.^{9,8} We list the results by Adams and Gardner⁸ after subtracting 12 cm^{-1} from their values. The vibrational frequencies in the figures are presented species by species. The dashed lines relating the calculated frequencies of the isolated ring to those of benitoite are derived by gradually increasing Ba and Ti interactions with the ring. Those relations clearly determine the Davydov pairs. In every case, the calculated frequency is sufficiently close to an observed mode of the same species to permit an unambiguous assignment. In particular, we are able to clearly identify modes which are due primarily to the internal vibration of the ring. The rest of the observed modes are then primarily either translational or rotational motions of the ring, or translations of the Ba and Ti ions. These external modes are described briefly next to the corresponding lines in the figures. Roughly

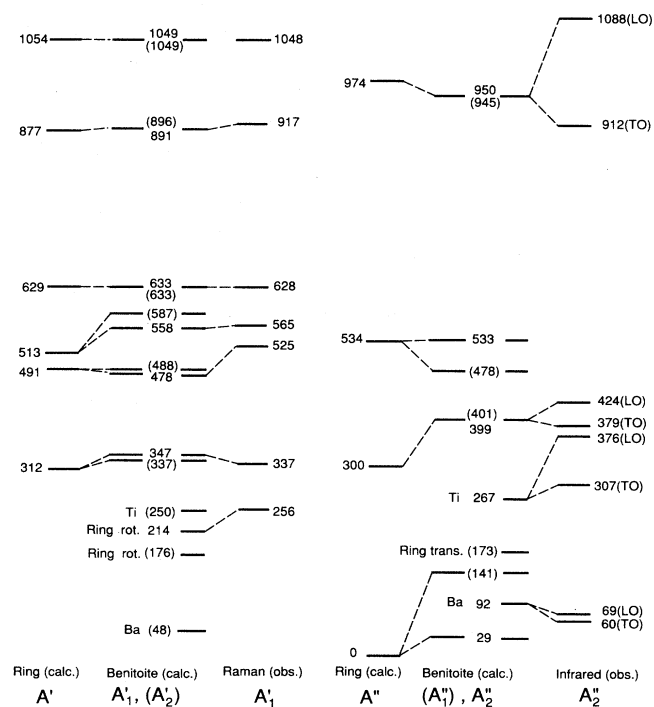


FIG. 3. The vibrational frequencies of nondegenerate optical modes of the ring and benitoite. The solid lines represent the vibrational frequencies and each of their heights is proportional to the corresponding value of the vibrational frequency. The Raman and infrared spectra are obtained from Refs. 9 and 8, respectively. The dashed lines relating the solid lines are our interpretation.

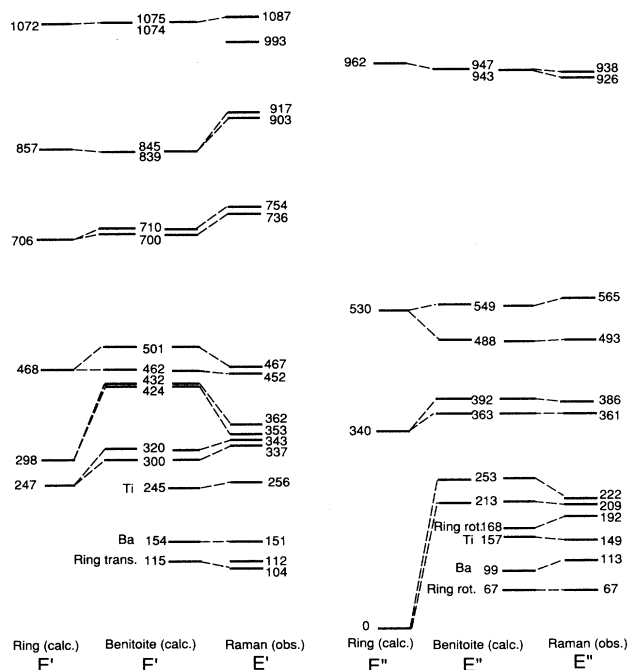


FIG. 4. The vibrational frequencies of doubly degenerate optical modes of the ring and benitoite. The solid lines represent the vibrational frequencies and each of their heights is proportional to the corresponding value of the vibrational frequency. The Raman spectra are obtained from Ref. 9. The dashed lines relating the solid lines are our interpretation.

speaking, the vibrational modes internal to the ring have frequencies above 300 cm^{-1} , while the external modes occur below this frequency.

The A'_1 and A'_2 species are shown in Fig. 3. Table I indicates that seven A'_1 frequencies are expected, and all are actually observed. The calculated ring breathing mode at 347 cm^{-1} matches our observed frequency of 337 cm^{-1} , but is not observed by Adams and Gardner. Although the modes of species A'_2 cannot be observed, they are related to the A'_1 modes by Davydov splittings which we find to be small. The good agreement with experiment for the A'_1 modes thus leads us to expect that the calculation is accurate for A'_2 as well.

The A''_1 and A''_2 species are shown in Fig. 3. Adams and Gardner reported both the estimated values and Kramers-Kronig values of A''_2 frequencies. Their estimated values are given in the figure. Six frequencies are expected in the infrared spectra, but only four are observed. The calculated frequency at 29 cm^{-1} may be too low to be observed. The mode predicted at 533 cm^{-1} may be too weak to be observed. The mean-square difference between the calculated and observed frequencies is greater for A''_2 than for A'_1 species. This is to be expected, since the calculation neglects the long-range Coulomb interactions which produce a splitting of longitudinal (LO) and transverse (TO) modes in this species. The calculated frequencies are generally in better agreement with

the observed TO frequencies. This, too, is expected since, depending on the detailed treatment of the local electric field, the effects of the Coulomb interactions will appear predominantly or exclusively in the LO modes. Despite the fact that frequencies of this species are not used in the fitting, the calculation is able to predict the observed TO frequencies with a worst-case error of 30 cm⁻¹.

The E' species are shown in Fig. 4. The vibrational spectra of E' symmetry also exhibit LO-TO shifts. We show only the observed TO modes, since they agree better with the calculated frequencies. Fifteen frequencies of E' species are expected and more than this number are observed. As in the A'_2 case, the agreement between theory and experiment for E' is poorer than for the A'_1 and E'' species. The observed frequency at 993 cm⁻¹ does not appear to have any counterpart in our calculation. It is too far from 1087 cm⁻¹ to be considered as its counterpart in a Davydov pair. It may be, however, due to a combination or overtone. Among the various possibilities of having E' species from combining two different species, the combination of 938 cm⁻¹ (E'') with 67 cm⁻¹ (E'') produces 1005 cm⁻¹ ($A'_1 + A'_2 + E'$), which is the closest to the observed frequency 993 cm⁻¹ (E'). In terms of modes, it is the combination of ring vibration with a lattice vibration. The calculated frequency of 115 cm⁻¹ is related with the observed frequency of 104 cm⁻¹ rather than 112 cm⁻¹, simply because the intensity of the line at 104 cm⁻¹ is stronger than that at 112 cm⁻¹. The vibrational mode near 750 cm⁻¹ is known as the "ring band,"⁶ since the infrared line is very strong and is a characteristic feature in the spectra of cyclosilicates containing rings. On the other hand, weak Raman lines at 754 cm⁻¹ and 736 cm⁻¹ are observed.

The E'' species are shown in Fig. 4. Twelve modes of E'' symmetry are expected in the Raman spectra. All of them are observed.⁹ The observed frequency at 169 cm⁻¹ by Adams and Gardner is close to the calculated frequency of 168 cm⁻¹, but is not seen in our data.⁹ The calculated frequency at 168 cm⁻¹ could correspond to the 169 cm⁻¹ line observed by Adams and Gardner or more probably, to the stronger 192 cm⁻¹ line observed in both sets of data.^{8,9} We suspect that the line observed at 169 cm⁻¹ by Adams and Gardner may not be one of the fundamental modes.

V. DISCUSSION

Our calculation yields the normal modes corresponding to each of the calculated frequencies. Figures 5 and 6 show some of these normal modes. Only half of the crystal structure (Fig. 1) is shown because each mode is either symmetric or antisymmetric with respect to rotation about the twofold axis. Figure 5 illustrates several high-frequency modes which are essentially ring vibrations. Also shown is the correspondence between the calculated normal mode of the isolated ring (first row) and its counterpart in the crystal (second row). The response of the surrounding atoms to the vibration of the ring can also be seen. In general, the higher the mode frequency, the more the normal mode of the crystal lattice resembles its "molecular" counterpart in the isolated ring. Likewise,

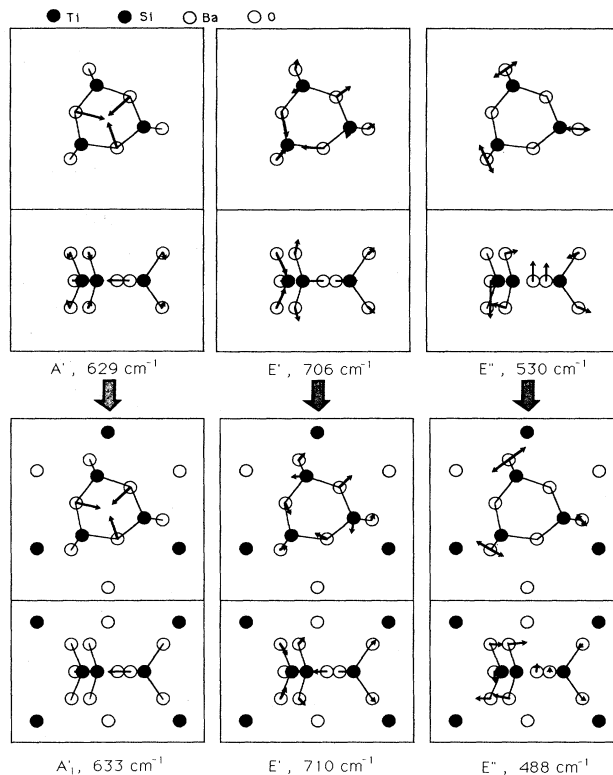


FIG. 5. Primarily vibrational modes of the ring and benitoite. The normal mode of the isolated ring (first row) is related with its counterpart in benitoite (second row). The diagrams in the top and bottom box are the top and side views, respectively. The length of the arrow is drawn to scale, indicating the relative amplitude of the motion of each atom for a normal mode.

the high-frequency modes involve relatively less motion of the Ti and Ba ions. Figure 6 shows several low-frequency modes which are essentially external to the ring, corresponding to rigid rotation or translation of the ring or to translation of the Ti ions.

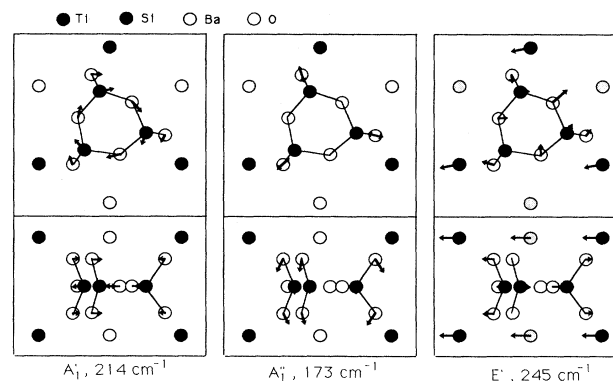


FIG. 6. Primarily external modes of benitoite. The diagrams in the top and bottom boxes are the top and side views, respectively. The length of the arrow is drawn to scale, indicating the relative amplitude of the motion of each atom for a given normal mode.

The normal mode analysis gives us confidence in our interpretation⁹ of the observed spectra, even where our assignments differ from those of Adams and Gardner.⁸ In particular, our identification of the pairs produced by Davydov splitting is highly reliable since it is based on a quantitative correlation of the normal modes of the isolated ring with those of the crystal.

A particularly questionable assignment by Adams and Gardner⁸ is that of the 738 cm^{-1} (E') and 492 cm^{-1} (E') modes as due primarily to Ti-O(2) bond stretching.⁸ Our analysis identifies these modes as internal to the rings. While we do obtain some Ti motion in modes with frequencies as high as 750 cm^{-1} , the interpretation of Ref. 8 requires a much larger value of the Ti-O(2) bond-stretching force constant than would be consistent with our calculations. This force constant plays another crucial role in the analysis. Our results are consistent with the conventional view² that the Ti-O bond-stretching interaction is much stronger than the Ba-O bond stretching. If, on the other hand, we fit our model to the frequencies reported in Ref. 8 without shifting the data by 12 cm^{-1} in order to bring them into agreement with our measurements,⁹ the result is a Ti-O bond-stretching force which is weaker by a factor of 3 than the Ba-O bond stretching. A similar problem arises if we neglect LO-TO shifts and include the observed frequencies of E' species in the fitting.

In Sec. III, we demonstrated a method which can extract the vibrational frequencies of the isolated ring from spectra measured on the crystal. This is valuable because knowledge of the spectrum of the Si_3O_9 ring is an important key to understanding the spectra of amorphous silicates containing rings.⁴ As shown in Figs. 3 and 4, the frequency difference between corresponding modes in the isolated ring and the crystal increases as the mode frequency decreases. For example, the E' mode at 247 cm^{-1} in the ring corresponds to the 310 cm^{-1} mode of the crystal, a shift of 63 cm^{-1} . Sharma, Philpotts, and Matson⁴ related the vibrational spectra of the smallest ring structures in some tectosilicates to those of the isochemical glasses, where the rings can be considered as more or less isolated molecules. They found, in particular, that the vibrational frequencies of crystalline $\text{LiAlSi}_2\text{O}_6$ -II, $\text{NaAlSi}_3\text{O}_8$, and $\text{CaAl}_2\text{Si}_3\text{O}_8$ are higher than those of the corresponding glasses by about 20 cm^{-1} . The effect is even more dramatic in our calculations, probably because we compare the crystal with an ideal, completely isolated ring, rather than a glass where there remains some coupling between the ring and its environment. These considerations suggest that information of the type presented in Secs. III and IV can be used to understand the vibrational spectra of amorphous silicates. As we continue to analyze the spectra of additional cyclosilicates,

as well as silicates having other types of polymerization, we expect to obtain further insight into the behavior of silicate glasses.

Finally, we consider the peculiar behavior of the A'_1 mode observed at 628 cm^{-1} . As shown in Fig. 6, this is a breathing mode in which only O(1) moves. Galeener, Barrio, Martinez, and Elliott²⁸ have pointed out that in a glass a mode of this type would be essentially decoupled from its environment. They attribute the sharp line at 606 cm^{-1} in $\nu\text{-SiO}_2$ to such a breathing mode of a planar three-ring. Our results are consistent with this analysis. It should be noted that the 628 cm^{-1} line is not particularly intense in the Raman spectrum of benitoite. It is possible that the prominence of the corresponding feature in the spectrum of SiO_2 glass is due entirely to its decoupling from the amorphous network, which prevents it from being broadened to the same extent as the other vibrations. The fact that the decoupled ring breathing mode in benitoite is roughly 20 cm^{-1} higher in energy than its counterpart in $\nu\text{-SiO}_2$ is perhaps not surprising in light of the discussion in the previous paragraph. Studies of the analogous modes in other cyclosilicates are needed in order to determine how much variation in frequency, intensity, and linewidth will occur in various structures. The results will help to establish whether or not the behavior of this decoupled mode is in some sense universal in silicates.

We have presented a normal mode calculation for the cyclosilicate mineral benitoite based on a correlation of the vibrational properties of the Si_3O_9 ring with those of the crystal. Despite the simplicity of the valence-force potential used (and the absence of long-range Coulomb interactions) the results enable us to give a complete description of the observed infrared and Raman spectra. More importantly, they permit us to identify modes characteristic of the Si_3O_9 ring, study their coupling to the rest of the crystal lattice, and begin to infer the behavior of these modes when the ring is embedded in the random network of a glass. Studies of other silicate minerals are in progress, with the aim of taking systematic advantage of this strategy to expand our understanding of the vibrational and structural properties of silicate glasses.

ACKNOWLEDGMENTS

The authors are grateful to C. I. Merzbacher who measured the infrared reflectance spectra of benitoite upon our request. One of the authors (C.C.K.) thanks L. Boyer for his help in the initial stage of the lattice dynamics calculation. D. A. McKeown was supported in part by Office of Naval Research Contract No. N00014-89-5-3010 at Howard University. C. C. Kim acknowledges the financial support of the National Research Council.

*On leave from National Institute of Standards and Technology, Gaithersburg, MD 20899.

¹F. Liebau, *Structural Chemistry of Silicates* (Springer-Verlag, New York, 1985).

²A. N. Lazarev, *Vibrational Spectra and Structure of Silicates* (Consultants Bureau, New York, 1972).

³P. F. McMillan and A. M. Hofmeister, *Rev. Mineral.* **18**, 141 (1988).

- ⁴S. K. Sharma, J. A. Philpotts, and D. W. Matson, *J. Non-Cryst. Solids* **85**, 403 (1985).
- ⁵K. Fischer, *Z. Kristallogr.* **129**, 222 (1969).
- ⁶F. Matossi and H. Krüger, *Z. Phys.* **99**, 1 (1936).
- ⁷W. P. Griffith, *J. Chem. Soc. A* 1372 (1969).
- ⁸D. M. Adams and I. R. Gardner, *J. Chem. Soc. Dalton Trans.* 316 (1976).
- ⁹D. McKeown, M. I. Bell, and C. C. Kim (unpublished).
- ¹⁰C. I. Merzbacher (private communication).
- ¹¹F. Matossi, *J. Chem. Phys.* **17**, 679 (1949).
- ¹²B. D. Saksena, K. C. Agarwal, and G. S. Jauhri, *Trans Faraday Soc.* **59**, 276 (1963).
- ¹³A. S. Davydov, *Theory of Molecular Excitons* (McGraw-Hill, New York, 1962).
- ¹⁴W. Hayes and R. Loudon, *Scattering of Light by Crystals* (Wiley, New York, 1978).
- ¹⁵M. Born and K. Huang, *Dynamic Theory of Crystal Lattices* (Oxford University Press, Oxford, 1954).
- ¹⁶G. Turrell, *Infrared and Raman Spectra of Crystals* (Academic, London, 1972).
- ¹⁷J. R. Hardy and A. M. Karo, *The Lattice Dynamics and Statics of Alkali Halide Crystals* (Plenum, New York, 1979).
- ¹⁸E. B. Wilson, J. C. Decius, and P. C. Cross, *Molecular Vibrations* (McGraw-Hill, New York, 1955).
- ¹⁹Quantum Chemistry Program Exchange, No. QCMP-012, Chemistry Department, Indiana University, Bloomington, Indiana 47401.
- ²⁰G. Herzberg, *Infrared and Raman Spectra of Polyatomic Molecules* (Van Nostrand, New York, 1946), Chap. 2.
- ²¹L. Boyer, *J. Comput. Phys.* **16**, 167 (1974).
- ²²L. Boyer (private communication).
- ²³V. Heine, *Group Theory in Quantum Mechanics* (Pergamon, New York, 1960), p. 119.
- ²⁴W. Zachariasen, *Z. Kristallogr.* **74**, 139 (1930).
- ²⁵O(2) in one tetrahedron indeed interacts with O(2) in another tetrahedron through Ba and Ti ions in benitoite.
- ²⁶G. Venkataraman and V. C. Sahni, *Rev. Mod. Phys.* **42**, 409 (1970).
- ²⁷H. Kanamori, S. Hayashi, and Y. Ikeda, *J. Phys. Soc. Jpn.* **36**, 511 (1974).
- ²⁸F. L. Galeener, R. A. Barrio, E. Martinez, and R. J. Elliott, *Phys. Rev. Lett.* **53**, 2429 (1984).